

FREQUENCY DOMAIN ADAPTIVE ALGORITHMS FOR STEREOPHONIC ACOUSTIC ECHO CANCELLATION EMPLOYING TAP SELECTION

Andy W.H. Khong and Patrick A. Naylor

{andy.khong, p.naylor}@imperial.ac.uk

Department of Electrical and Electronic Engineering, Imperial College London, UK

ABSTRACT

The use of a tap-selection approach for stereophonic acoustic echo cancellation in frequency domain adaptive algorithms is investigated. We first provide an analysis showing how the exclusive-maximum (XM) tap-selection scheme can improve the conditioning of the covariance matrix, hence improving convergence performance. We then show how the XM tap-selection can be extended to the frequency domain adaptive structure by considering the frequency least-mean-square (FLMS) algorithm which employs a 50% input overlap. We also consider the case of XM tap-selection under any arbitrary overlapping factor. Simulation results show approximately 3-6 dB improvement in convergence compared to existing frequency domain adaptive algorithms.

1. INTRODUCTION

In hands-free teleconferencing systems, stereophonic transmission can provide telepresence by enhancing source localization. The stereophonic acoustic echo canceller (SAEC) such as shown in Fig. 1, suppresses the echo returned to the transmission room so as to enable undisturbed communication between the rooms.

A serious problem encountered in stereophonic systems is the non-uniqueness problem [1] where the tap-input covariance matrix \mathbf{R} is highly ill-conditioned for practical systems. This is due to the high coherence between the two input signals $x_1(n)$ and $x_2(n)$ which in turn degrades the misalignment performance of adaptive algorithms in general. Many proposed solutions have since been introduced to decorrelate the two input signals [2][3] with the common aim of achieving interchannel decorrelation, hence improving the conditioning of \mathbf{R} without affecting the quality or stereophonic image of the speech.

Although selective-tap algorithms were originally proposed for complexity reduction in single channel AEC [4], a class of exclusive-maximum (XM) selective-tap algorithms was introduced recently for SAEC applications [5]. This XM tap-selection has been shown to improve the conditioning of \mathbf{R} such that, when used with the non-linear (NL) preprocessor [2], improved convergence per-

formance can be achieved compared to the use of NL-preprocessor alone. In Section 3, we first explain through mathematical analysis how XM tap-selection reduces the interchannel coherence which results in improved conditioning of \mathbf{R} . In Section 4, we then extend the XM tap-selection technique to the frequency domain least-mean-square (FLMS) algorithm [6] which employs a 50% input overlapping factor. We also consider the case of a generalized input overlapping factor scheme which is similar to the generalized multi-delay filter (GMDF $_{\alpha}$) [7], where $\alpha \geq 1$ is the overlap factor control between successive tap-input blocks. Simulation results in Section 5 compare the proposed XM-based algorithms employing the NL preprocessor with frequency based algorithms employing the NL preprocessor alone.

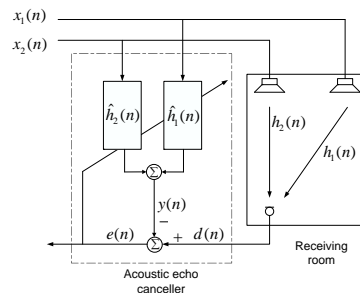


Figure 1: Simplified stereophonic acoustic echo cancellation system.

2. THE EXCLUSIVE MAXIMUM (XM) TAP-SELECTION

The exclusive-maximum (XM) tap-selection criterion [5] aims jointly to maximize the energy of the selected tap-inputs whilst minimizing the interchannel coherence at each iteration. This tap-selection addresses the minimum coherence condition by constraining tap-selections to be exclusive such that the same coefficient index may not be selected in both channels.

Defining L as the filter length such that $\mathbf{x}_j(n) = [x_j(n), \dots, x_j(n - L + 1)]^T$ for channels $j = 1, 2$ and

$$\mathbf{p}(n) = |\mathbf{x}_1(n)| - |\mathbf{x}_2(n)|, \quad (1)$$

the XM tap-selection matrix is $\mathbf{Q}(n) = \text{diag}\{\mathbf{q}_1(n), \mathbf{q}_2(n)\}$ such that at each iteration n , element u of $\mathbf{q}_1(n)$ and element v of $\mathbf{q}_2(n)$ are defined for $u, v = 1, 2, \dots, L$ as

$$\begin{aligned} q_{1,u} &= \begin{cases} 1 & p_u \in \{M \text{ maxima of } \mathbf{p}\} \\ 0 & \text{otherwise} \end{cases} \\ q_{2,v} &= \begin{cases} 1 & p_v \in \{M \text{ minima of } \mathbf{p}\} \\ 0 & \text{otherwise} \end{cases} \end{aligned} \quad (2)$$

Defining $\mathbf{x}(n) = [\mathbf{x}_1^T(n) \ \mathbf{x}_2^T(n)]^T$, $\mathbf{h}(n) = [\mathbf{h}_1^T(n) \ \mathbf{h}_2^T(n)]^T$ and μ as the adaptation step-size [8], the XM-NLMS weight update equation [5] is then given by

$$\hat{\mathbf{h}}(n+1) = \hat{\mathbf{h}}(n) + \mu \frac{\mathbf{Q}(n)\mathbf{x}(n)e(n)}{\|\mathbf{x}(n)\|_2^2 + \delta}, \quad (3)$$

where $\|\cdot\|_2^2$ and δ are defined as the squared l_2 -norm and regularization parameter respectively.

3. EFFECT OF XM TAP-SELECTION

3.1. Effect of XM tap-selection on interchannel coherence

We show the effect of XM tap-selection on interchannel coherence by first expressing the two channel covariance Toeplitz matrix as

$$\mathbf{R} = E\{\mathbf{x}(n)\mathbf{x}^T(n)\} = \begin{bmatrix} \mathbf{R}_{11} & \mathbf{R}_{12} \\ \mathbf{R}_{21} & \mathbf{R}_{22} \end{bmatrix}_{2L \times 2L}, \quad (4)$$

where we $E\{\cdot\}$ is the mathematical expectation operator. Letting $i = \sqrt{-1}$ and $r_{jk}(l)$ be the auto- and cross correlation coefficients for $j = k$ and $j \neq k$ respectively, we may express cross-power spectrum (across normalized frequency f) between two signals as

$$S_{jk}(f) = \sum_{l=-\infty}^{\infty} r_{jk}(l)e^{-i2\pi fl}, \quad f = 0, 1, \dots, L-1. \quad (5)$$

Noting that for $L \rightarrow \infty$, a Toeplitz matrix is asymptotically equivalent to a circulant matrix if its elements are absolutely summable [2], the autocorrelation matrix can then be decomposed as

$$\mathbf{R} = \begin{bmatrix} \mathbf{F}_{L \times L}^{-1} & \mathbf{0} \\ \mathbf{0} & \mathbf{F}_{L \times L}^{-1} \end{bmatrix} \begin{bmatrix} \mathbf{S}_{11} & \mathbf{S}_{12} \\ \mathbf{S}_{21} & \mathbf{S}_{22} \end{bmatrix} \begin{bmatrix} \mathbf{F}_{L \times L} & \mathbf{0} \\ \mathbf{0} & \mathbf{F}_{L \times L} \end{bmatrix} \quad (6)$$

where $\mathbf{0}$ is an $L \times L$ dimension null matrix, $\mathbf{F}_{L \times L}$ is the Fourier matrix with elements $F_{pq} = e^{-i2\pi pq/L}$ for $p, q = 0, 1, \dots, L-1$ and

$$\mathbf{S}_{jk} = \text{diag}\{S_{jk}(0), \dots, S_{jk}(L-1)\}, \quad j, k = 1, 2. \quad (7)$$

Using (5), the squared interchannel coherence function for the f th frequency bin can be expressed as

$$|\gamma(f)|^2 = \frac{|S_{12}(f)|^2}{S_{11}(f)S_{22}(f)}, \quad f = 0, 1, \dots, L-1. \quad (8)$$

Defining $\tilde{\mathbf{x}}_j = \mathbf{Q}_j(n)\mathbf{x}_j(n)$ for channels $j = 1, 2$, the reduction of interchannel coherence due to the exclusive tap-selection can now be observed by noting that the cross-correlation function

$$r_{12}(0) = r_{21}(0) = E\{\tilde{x}_1(n)\tilde{x}_2(n)\} = 0, \quad (9)$$

since by virtue of the exclusive tap-selection, we have $\mathbf{Q}_1(n) \odot \mathbf{Q}_2(n) = \mathbf{Q}_1(n)\mathbf{Q}_2(n) = \mathbf{0}$ where \odot is defined as the Schür product. In addition to (9), we also note that $r_{12}(l)$ and $r_{21}(l)$ in (5) is sparsified by $\mathbf{Q}(n)$. Consequently, $|S_{12}(f)|^2$ and hence the interchannel coherence $|\gamma(f)|^2$ as defined in (8) is reduced accordingly.

3.2. Effect of XM tap-selection on conditioning of \mathbf{R}

We now show the improvement in the conditioning of \mathbf{R} due to the reduction in interchannel coherence brought about by XM tap-selection as explained in the previous Section. Defining $\text{tr}\{\cdot\}$ as the trace operator, the E-norm of a $2L \times 2L$ matrix is then defined as [9]

$$\|\mathbf{R}\|_E = \left[\frac{1}{2L} \text{tr}\{\mathbf{R}^T \mathbf{R}\} \right]^{1/2}. \quad (10)$$

Using the relation $\mathbf{R}^{1/2} = \mathbf{U}\Lambda^{1/2}\mathbf{U}^T$, where $\Lambda = \text{diag}\{\bar{\lambda}_0, \bar{\lambda}_1, \dots, \bar{\lambda}_{2L-1}\}$ containing the eigenvalues of \mathbf{R} , it follows that

$$\|\mathbf{R}^{1/2}\|_E = \left[\frac{1}{2L} \text{tr}\{\mathbf{R}\} \right]^{1/2}, \quad \|\mathbf{R}^{-1/2}\|_E = \left[\frac{1}{2L} \text{tr}\{\mathbf{R}^{-1}\} \right]^{1/2} \quad (11)$$

which results in the E-norm condition number

$$\chi_E[\mathbf{R}^{1/2}] = \|\mathbf{R}^{1/2}\|_E \|\mathbf{R}^{-1/2}\|_E. \quad (12)$$

Defining

$$\mathbf{S} = \begin{bmatrix} \mathbf{S}_{11} & \mathbf{S}_{12} \\ \mathbf{S}_{21} & \mathbf{S}_{22} \end{bmatrix}, \quad (13)$$

we may compute $\text{tr}\{\mathbf{R}\}$ using (6), (11) and the relation $\text{tr}\{\mathbf{AB}\} = \text{tr}\{\mathbf{BA}\}$, such that

$$\text{tr}\{\mathbf{R}\} = \sum_{l=0}^{L-1} [S_{11}(l) + S_{22}(l)]. \quad (14)$$

Using (6), and following similar approach as [2], we now compute $\text{tr}\{\mathbf{R}^{-1}\} = \text{tr}\{\mathbf{S}^{-1}\}$ by first expressing \mathbf{S}^{-1} as

$$\mathbf{S}^{-1} = \begin{bmatrix} \mathbf{S}_{11}^{-1} & \mathbf{0}_{L \times L} \\ \mathbf{0}_{L \times L} & \mathbf{S}_{22}^{-1} \end{bmatrix} \begin{bmatrix} \mathbf{I}_{L \times L} & -\mathbf{S}_{12}\mathbf{S}_{22}^{-1} \\ -\mathbf{S}_{21}\mathbf{S}_{11}^{-1} & \mathbf{I}_{L \times L} \end{bmatrix}, \quad (15)$$

where $\mathbf{I}_{L \times L}$ is an $L \times L$ identity matrix and the submatrices

$$\mathbf{S}_1 = [\mathbf{I}_{L \times L} - \mathbf{S}_{12}^2(\mathbf{S}_{11}^{-1}\mathbf{S}_{22}^{-1})]\mathbf{S}_{11}, \quad (16)$$

$$\mathbf{S}_2 = [\mathbf{I}_{L \times L} - \mathbf{S}_{12}^2(\mathbf{S}_{11}^{-1}\mathbf{S}_{22}^{-1})]\mathbf{S}_{22}. \quad (17)$$

We may now express the diagonal matrices \mathbf{S}_1^{-1} and \mathbf{S}_2^{-1} of (15) as

$$\mathbf{S}_1^{-1} = [\mathbf{I}_{L \times L} - |\Gamma|^2]^{-1}\mathbf{S}_{11}^{-1}, \quad (18)$$

$$\mathbf{S}_2^{-1} = [\mathbf{I}_{L \times L} - |\Gamma|^2]^{-1}\mathbf{S}_{22}^{-1}, \quad (19)$$

where $|\Gamma|^2 = \text{diag}\{|\gamma(0)|^2, |\gamma(1)|^2, \dots, |\gamma(L-1)|^2\}$ with the elements as defined in (8). Using (15), (18) and (19), we can now simplify $\text{tr}\{\mathbf{R}^{-1}\} = \text{tr}\{\mathbf{S}^{-1}\}$ hence giving

$$\text{tr}\{\mathbf{R}^{-1}\} = \sum_{l=0}^{L-1} [1 - |\gamma(l)|^2]^{-1} [S_{11}^{-1}(l) + S_{22}^{-1}(l)]. \quad (20)$$

Substituting (14) and (20) into (12), we finally obtain the relationship between interchannel coherence and E-norm condition number of \mathbf{R} given as

$$\chi_E^2[\mathbf{R}^{1/2}] = \frac{1}{4L^2} \left[\sum_{l=0}^{L-1} [S_{11}(l) + S_{22}(l)] \right] \times \left[\sum_{l=0}^{L-1} [1 - |\gamma(l)|^2]^{-1} [S_{11}^{-1}(l) + S_{22}^{-1}(l)] \right]. \quad (21)$$

We can now see that due to the exclusive tap-selection, the reduction in interchannel coherence in (9) will reduce the E-norm condition number of \mathbf{R} in (21) and hence improved misalignment performance of XM-based algorithms [5] is expected.

4. FREQUENCY DOMAIN ADAPTIVE ALGORITHMS

We now extend the XM tap-selection to the frequency domain LMS (FLMS) algorithm [6] by first defining m as the block time index. The j th channel tap-input sequence of dimension $2L \times 1$ (with 50% overlap factor) is then defined as

$$\mathbf{x}_j(m) = [x_j(mL - L), \dots, x_j(mL + L - 1)]^T. \quad (22)$$

For tap-selection, we first express $\mathbf{x}_j(m)$ as

$$\mathbf{x}_j(m) = [\mathbf{x}_{a,j}^T(m-1) \ \mathbf{x}_{a,j}^T(m)]^T, \quad (23)$$

where $\mathbf{x}_{a,j}(m) = [x(mL), \dots, x(mL + L - 1)]^T$. We may then subselect the tap-input vectors by $\tilde{\mathbf{x}}_{a,j}(m) = \mathbf{Q}_j(m)\mathbf{x}_{a,j}(m)$ where $\mathbf{Q}_j(m) = \text{diag}\{\mathbf{q}_j(m)\}$ such that (2) is satisfied and

$$\mathbf{p}(m) = |\mathbf{x}_{a,1}(m)| - |\mathbf{x}_{a,2}(m)|. \quad (24)$$

Hence for each block iteration m , the subselected overlapped tap-input vector is given by

$$\tilde{\mathbf{x}}_j(m) = [\tilde{\mathbf{x}}_{a,j}^T(m-1) \ \tilde{\mathbf{x}}_{a,j}^T(m)]^T. \quad (25)$$

Using (25) and defining

$$\begin{aligned} \mathbf{y}(m) &= [y(mL), \dots, y(mL + L - 1)]^T, \\ \mathbf{d}(m) &= [d(mL), \dots, d(mL + L - 1)]^T, \\ \mathbf{e}(m) &= \mathbf{d}(m) - \mathbf{y}(m), \end{aligned}$$

the FLMS employing XM tap-selection can then be expressed as shown in Table 1 where $*$ is the complex conjugate operator and: $\sigma_x^2 = E\{\mathbf{x}^T(m)\mathbf{x}(m)\}$, $\underline{\mathbf{d}}(m) =$

Table 1: XM-FLMS

for each channel $j = 1, 2$	
λ	$= [1 - 1/(3L)]^L, \kappa = \mu(1 - \lambda)$
$P_i(0)$	$= \sigma_x^2, i = 0, \dots, 2L - 1$
$\tilde{\mathbf{x}}_{a,j}(m)$	$= \mathbf{Q}_j(m)\mathbf{x}_{a,j}(m)$
$\tilde{\mathbf{x}}_j(m)$	$= [\tilde{\mathbf{x}}_{a,j}^T(m-1) \ \tilde{\mathbf{x}}_{a,j}^T(m)]^T$
$\tilde{\mathbf{x}}_j(m)$	$= \text{diag}\{\mathbf{F}_{2L \times 2L}\tilde{\mathbf{x}}_j(m)\}$
$\underline{\mathbf{x}}_j(m)$	$= \text{diag}\{\mathbf{F}_{2L \times 2L}\mathbf{x}_j(m)\}$
$\mathbf{y}(m)$	$= \mathbf{G}^{01} \sum_{j=1}^2 \underline{\mathbf{x}}_j(m)\hat{\mathbf{h}}_j(m)$
$\underline{\mathbf{e}}(m)$	$= \underline{\mathbf{d}}(m) - \mathbf{y}(m)$
$\mathbf{P}(m)$	$= \lambda\mathbf{P}(m-1) + (1 - \lambda) \sum_{j=1}^2 \mathbf{x}_j^*(m)\mathbf{x}_j(m)$
$\mu(m)$	$= \kappa \times [\text{diag}\{\mathbf{P}(m)\}]^{-1}$
$\hat{\mathbf{h}}_j(m+1)$	$= \hat{\mathbf{h}}_j(m) + \mathbf{G}^{10}\mu(m)\tilde{\mathbf{x}}_j^*(m)\underline{\mathbf{e}}(m)$

$$\begin{aligned} \mathbf{F}_{2L \times 2L} \begin{bmatrix} \mathbf{0}_{L \times 1} \\ \mathbf{d}(m) \end{bmatrix}, \mathbf{y}(m) &= \mathbf{F}_{2L \times 2L} \begin{bmatrix} \mathbf{0}_{L \times 1} \\ \mathbf{y}(m) \end{bmatrix}, \hat{\mathbf{h}}(m) = \\ \mathbf{F}_{2L \times 2L} \begin{bmatrix} \hat{\mathbf{h}}(m) \\ \mathbf{0}_{L \times 1} \end{bmatrix}, \underline{\mathbf{e}}(m) &= \mathbf{F}_{2L \times 2L} \begin{bmatrix} \mathbf{0}_{L \times 1} \\ \mathbf{e}(m) \end{bmatrix}, \mathbf{W}^{01} = \\ \begin{bmatrix} \mathbf{0}_{L \times L} & \mathbf{0}_{L \times L} \\ \mathbf{0}_{L \times L} & \mathbf{I}_{L \times L} \end{bmatrix}, \mathbf{W}^{10} &= \begin{bmatrix} \mathbf{I}_{L \times L} & \mathbf{0}_{L \times L} \\ \mathbf{0}_{L \times L} & \mathbf{0}_{L \times L} \end{bmatrix}, \mathbf{G}^{01} = \\ \mathbf{F}_{2L \times 2L} \mathbf{W}^{01} \mathbf{F}_{2L \times 2L}^{-1} \text{ and } \mathbf{G}^{10} &= \mathbf{F}_{2L \times 2L} \mathbf{W}^{10} \mathbf{F}_{2L \times 2L}^{-1}. \end{aligned}$$

Instead of 50% overlapping factor as shown in (23), we may further consider extending the XM tap-selection to the two channel FLMS algorithm [2] using any arbitrary overlapping factor. This is similar to the GMDF α structure [7] where improved convergence rate can be achieved by the successive tap-input frames overlapping controlling factor $\alpha \geq 1$ such that for $\alpha = 1$, a 50% overlap between successive input blocks is obtained as shown in (23). In addition, the single channel GMDF α algorithm reduces the delay inherent in frequency domain approaches by partitioning the adaptive filter into K blocks each of size N such that $L = KN$. In this paper, as our aim is to introduce tap-selection for any arbitrary $\alpha \geq 1$, we shall only consider the case where $K = 1$. To incorporate the XM tap-selection into any arbitrary overlapping factor, we first note that $x_j(n)$, $j = 1, 2$, is partitioned into overlapping sections each with size $2L$. At each block iteration m , the tap-input sequence for the j th channel can be denoted by

$$\mathbf{x}_j(m) = [x_j(m; 0), \dots, x_j(m; 2L - 1)]^T, \quad (26)$$

$$x_j(m; \tau) = x(\tau + mL/\alpha - L), \quad (27)$$

where $\tau = 0, 1, \dots, 2L - 1$ are the tap-input vector indices for this arbitrary overlapping factor algorithm for which we shall denote FLMS α . Using these relationships, we can see that for $\alpha = 1$, we obtain the FLMS algorithm. Similar to (1), we can then define a $2L \times 1$ difference vector

$$\mathbf{p}(m) = |\mathbf{x}_1(m)| - |\mathbf{x}_2(m)|, \quad (28)$$

where $\mathbf{x}_j(m)$, $j = 1, 2$ for this arbitrary overlapping factor case is as defined in (26) and (27). For the XM tap-selection, we employ the criterion given in (2). Consequently, the tap-selection matrix for each channel is a $2L \times 2L$ matrix which results in a subselected tap-input vector $\mathbf{Q}_j(m)\mathbf{x}_j(m)$.

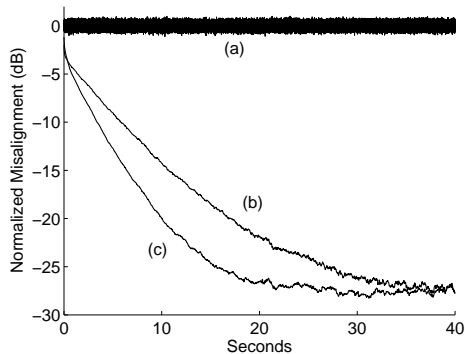


Figure 2: (a) WGN Signal and Normalized Misalignment for (b) NL-FLMS and (c) XMNL-FLMS.

5. SIMULATION RESULTS

Similar to that of the time-domain algorithms [5], the XM tap-selection relies on the existence of a unique solution introduced by the NL-preprocessor. We shall denote the use of XM tap-selection in combination with NL-preprocessor as XMNL. In all our simulations, the impulse responses of the transmission and receiving rooms are generated using the method of images and a non-linearity factor of 0.5 is used [2]. White Gaussian noise is added to the desired signal such that an SNR of 30 dB is achieved. Figure 2 shows simulation result for the FLMS-based adaptive algorithms using 50% input overlapping factor. The step-sizes of $\mu = 1$ and $\mu_{XM} = 0.705$ are used such that both algorithms achieve approximately the same final misalignment. The unknown impulse responses and adaptive filters are 800 and 256 respectively. We note that XMNL-FLMS achieves approximately 6 dB improvement in misalignment compared to the NL-FLMS algorithm.

Figure 3 shows simulation result for the arbitrary overlapping factor based algorithms where we have used an arbitrary chosen overlapping factor of $\alpha = 4$ for both the NL-FLMS $_{\alpha}$ and XMNL-FLMS $_{\alpha}$ algorithms. For this speech input example, the impulse responses and adaptive filters were of length 1024 and 512 respectively. We see that the XMNL-FLMS $_{\alpha}$ algorithm shows an additional 3 – 4 dB improvement in convergence rate compared to NL-FLMS $_{\alpha}$ without tap-selection.

6. CONCLUSION

XM tap-selection has been shown to reduce the interchannel coherence by exploiting the frequency domain quantities. We have further extended the XM tap-selection to frequency-domain adaptive algorithms. The XMNL based algorithms have shown improved performance compared to the use of NL-preprocessor alone.

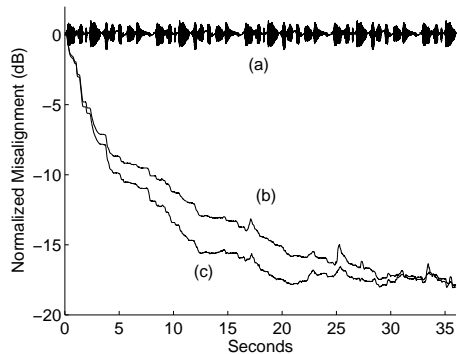


Figure 3: (a) Speech Signal and Normalized Misalignment for (b) NL-FLMS $_{\alpha}$ and (c) XMNL-FLMS $_{\alpha}$ with overlapping factor $\alpha = 4$.

7. ACKNOWLEDGEMENT

The authors would like to thank Prof. Jacob Benesty for his helpful comments and implementation of the two channel GMDF $_{\alpha}$ algorithm [2].

8. REFERENCES

- [1] J. Benesty, D. R. Morgan, and M. M. Sondhi, "A better understanding and an improved solution to the specific problems of stereophonic acoustic echo cancellation," *IEEE Trans. Speech Audio Processing*, vol. 6, no. 2, pp. 156–165, Mar. 1998.
- [2] J. Benesty, T. Gänslér, D. R. Morgan, M. M. Sondhi, and S. L. Gay, *Advances in Network and Acoustic Echo Cancellation*, Springer, 2001.
- [3] S. Shimauchi and S. Makino, "Stereo projection echo canceller with true echo path estimation," in *Proc. IEEE Int. Conf. Acoustics Speech Signal Processing*, 1995, vol. 5, pp. 3059–3062.
- [4] T. Aboulnasr and K. Mayyas, "Complexity reduction of the NLMS algorithm via selective coefficient update," *IEEE Trans. Signal Processing*, vol. 47, no. 5, pp. 1421–1424, 1999.
- [5] A. W. H. Khong and P. A. Naylor, "A family of selective-tap algorithms for stereo acoustic echo cancellation," in *Proc. IEEE Int. Conf. Acoustics Speech Signal Processing*, Mar. 2005, vol. 3, pp. 133–136.
- [6] E. Ferrara, "Fast implementations of LMS adaptive filters," *IEEE Trans. Acoust., Speech, Signal Processing*, vol. 28, pp. 474–475, 1980.
- [7] E. Moulines, O. A. Amrane, and Y. Grenier, "The generalized multidelay adaptive filter: Structure and convergence analysis," *IEEE Trans. Signal Processing*, vol. 43, no. 1, pp. 14–28, Jan. 1995.
- [8] S. Haykin, *Adaptive Filter Theory*, Information and System Science. Prentice Hall, 4th edition, 2002.
- [9] J. Benesty and T. Gänslér, "A recursive estimation of the condition number in the RLS algorithm," in *Proc. IEEE Int. Conf. Acoustics Speech Signal Processing*, 2005, vol. 4, pp. 25–28.